https://doi.org/10.5194/bg-2021-69
Preprint. Discussion started: 7 April 2021

Biogeosciences Discussions

Partitioning carbon sources in a tropical watershed (Nyong River, Cameroon) between wetlands and terrestrial ecosystems – Do CO_2 emissions from tropical rivers offset the terrestrial carbon sink?

Moussa Moustapha[1], Loris Deirmendjian[2, 3], David Sebag[4, 5, 6], Jean-Jacques Braun[2, 3, 7, 8], Stéphane Audry[2], Henriette Ateba Bessa[7], Thierry Adatte[9], Carole Causserand[2], Ibrahima Adamou[1], Benjamin Ngounou Ngatcha[1], Frédéric Guérin[2, 3].

[1]Université de Ngaoundéré, Faculté des Sciences, BP 454 Ngaoundéré, Cameroun
[2]Géosciences Environnement Toulouse (GET-Université de Toulouse, CNRS, IRD), Université de Toulouse Paul Sabatier, 14 Avenue Edouard-Belin, 31400 Toulouse, France
[3]IRD, UR 234, GET, 14 Avenue E. Belin, 31400, Toulouse, France
[4]Normandie Univ, UNIROUEN, UNICAEN, CNRS, M2C, 76000 Rouen, France
[5]HSM, IRD, CNRS, Université de Montpellier, Montpellier, France1
[6]IFPEN, Geosciences Dept, Rueil-Malmaison, France
[7]Institut de Recherches Géologiques et Minières/Centre de Recherches Hydrologiques, BP 4110, Yaoundé, Cameroun
[8]International Joint Laboratory DYCOFAC, IRGM-UY1-IRD, Rue Joseph Essono Balla, Quartier Elig Essono, BP 1857, Yaoundé, Cameroun
[9]Institut des Sciences de la Terre (ISTE), Université de Lausanne, GEOPOLIS, CH-1015 Lausanne, Switzerland

Correspondence to: Frédéric Guérin (frederic.guerin@ird.fr)

Abstract. We characterized the spatio-temporal dynamics of carbon (C) in rivers of the tropical Nyong catchment (South Cameroon). In 2016, we measured fortnightly at 6 locations along an upstream-downstream gradient from groundwater to the main stream of order 6, total alkalinity, dissolved inorganic C (DIC) used together with pH to compute pCO_2, dissolved and particulate organic C (DOC and POC) and total suspended matter. Forest, groundwater had low DOC content (<1 mg L^{-1}) as its leaching was probably prevented in the overlaying lateritic soils. Forest groundwater was supersaturated in CO_2 (~50 times the atmospheric value) because of the solubilisation of the CO_2 originating from soil respiration. Wetlands water exhibited higher DOC (>14 mg L^{-1}) and similar DIC concentrations than the forest groundwater. Surface runoff was considered negligible in the basin due to low slopes and high infiltration capacity of the soils, making wetlands and forest groundwater the two main sources of C for surface waters. The influence of wetlands on C dynamics in rivers was significant during periods of high waters when the hydrological connectivity between surface waters and wetlands was enhanced. On annual scale, wetlands exported 60% (15.4±7.2 t C km^{-2} yr^{-1}) of the total amount of C transferred laterally to surface waters, the remaining 40% (12.1±5.8 t C km^{-2} yr^{-1}) being transferred from forest groundwater. Heterotrophic respiration in rivers averaged 89 mmol m^{-2} d^{-1} whereas CO_2 degassing was 1260 mmol m^{-2} d^{-1}, which shows that it is unlikely that the river heterotrophic respiration was the main process sustaining CO_2 emission. The comparison of the hydrological export of terrestrial C via forest groundwater with the net terrestrial C sink in the Nyong watershed shows that only ~4% of the net terrestrial C sink reach the aquatic ecosystem. The carbon mass balance of the Nyong watershed highlights that attributing to a unique terrestrial source

https://doi.org/10.5194/bg-2021-69
Preprint. Discussion started: 7 April 2021


Biogeosciences Discussions

the whole amount of riverine carbon emitted to the atmosphere and exported to the ocean and ignoring the river–wetland connectivity can lead to the misrepresentation of C dynamics in tropical watersheds.

1 Introduction

Despite their small surface area worldwide (Allen and Pavelsky, 2018), inland waters have a disproportional role in the global carbon (C) cycle. They receive C from terrestrial ecosystems and export it to the atmosphere and the ocean (Cole et al., 2007; Ludwig et al., 1996; Meybeck, 1982). Terrestrial aquatic ecosystems are significant hotspots of C dioxide (CO_2) (e.g., Raymond et al., 2013) since inland waters are usually supersaturated in CO_2 and CH_4 compare to the overlying atmosphere. The dissolved CO_2 in riverine waters originates from internal metabolism (mainly heterotrophic decomposition of organic matter in the aquatic system itself) and from lateral external inputs (mainly groundwater and riparian wetlands) (Abril and Borges, 2019; Borges et al., 2015; Hotchkiss et al., 2015). Global inland waters emit 2.1 Pg CO_2 yr^{-1} to the atmosphere (Raymond et al., 2013). However, the dataset used by Raymond et al. (2013) is based on the CO_2 water partial pressure (pCO_2) calculated from pH and alkalinity (TA), which calculation method leads to overestimation of pCO_2 (up to 75 times), notably in low buffered, and high organic waters, such as boreal and tropical rivers (Abril et al., 2015). In addition, the most recent estimates of river areal extent by (Allen and Pavelsky, 2018) are higher by 44% than those used by Raymond et al. (2013), which should lead to an upward revision of CO_2 emissions from inland waters (Abril and Borges, 2019). At the global scale, the degassing of CO_2 from inland waters is of the same order of magnitude as the net terrestrial C sink (Drake et al., 2018). The quantification of dissolved C fluxes in inland waters originating from lateral hydrological inputs (i.e., soil and groundwater from well-drained terrestrial ecosystems vs. wetland from semi-aquatic ecosystems) is fundamental to close the riverine C budget at the catchment scale (Abril and Borges, 2019; Deirmendjian et al., 2018). Yet, lateral hydrological export of C from terrestrial ecosystems to inland waters has been under attention only in the last 10 years (Ciais et al., 2008; Cole and Caraco, 2001). However, the flux of C across the boundary between land and water cannot be determined experimentally at the global scale (Abril and Borges, 2019). Therefore, hydrological C export from terrestrial systems is usually estimated from the sum of the inputs and outputs of C entering or escaping inland waters (e.g., Cole et al., 2007), which does not allow to close the anthropogenic C budget in a whole watershed encompassing terrestrial ecosystems, rivers and wetlands (Abril and Borges, 2019). Abril and Borges (2019) showed that the hydrological C export necessary to balance the inland water C budget is 1.9–3.2 Pg C yr^{-1}, which corresponds to 75%–125% of the terrestrial C sink estimated by Ciais et al. (2013). The offset of the terrestrial C sink by inland waters is in discrepancy with atmospheric CO_2 inversions, terrestrial ecosystem models and forest inventories that all located a net terrestrial C sink at the global scale. As a result, at the global scale, it is unlikely that only the C exported laterally from land would sustain all C fluxes in inland waters. Indeed, at the plot scale, studies in temperate forest system that compare the net C sink with the hydrological C export showed that only a minor portion (~3%) of the terrestrial C is in fact exported laterally from land to the river network (Deirmendjian et al., 2018; Kindler et al., 2011). Abril and Borges (2019) proposed a new conceptual model of the global C cycle in inland waters, where part of the discrepancy between CO_2

https://doi.org/10.5194/bg-2021-69
Preprint. Discussion started: 7 April 2021

emissions estimates from inland waters and the hydrological export of C from terrestrial well-drained systems could be actually attributed to carbon transfer from wetlands to inland waters.

There is now consensus that tropical regions are hotspots of riverine C export and degassing (Borges et al., 2015a, 2019; Sawakuchi et al., 2014). Indeed, recent estimates of CO_2 emissions from tropical rivers (latitude < 25°) (Borges et al., 2015b) based on results in several African rivers (Borges et al., 2015a) and in the Amazon (Abril et al., 2014) is about 1.8±0.4 Pg C yr^{-1} . Noteworthy, the estimate of Borges et al. (2015a) is conservative since it does not account for lakes and extensive tropical wetlands that act as hotspots of biological productivity, which could fuel C emissions to the atmosphere from rivers to which they are connected (e.g., Abril et al., 2014; Abril and Borges, 2019; Borges et al., 2015). C global emissions estimates from inland waters are thus probably underestimated, due to the scarcity of data in the tropics, where inland waters exhibit higher emission rate per unit area compared to temperate ecosystems (Bastviken et al., 2011; Borges et al., 2015a).

The Nyong River basin (South Cameroon) has been subject to multidisciplinary hydro-biogeochemical monitoring since 1993. This basin belongs to the Critical Zone Observatories' network named Multiscale TROPIcal CatchmentS (M-TROPICS; https://mtropics.obs-mip.fr/), a long-term monitoring program of hydrobiogeochemical cycles in the tropics. The main objectives of this study are the description of the spatial (from groundwater to increasing stream order) and temporal (through the hydrological cycle) variations in C concentrations in the waters of the Nyong basin; and to decipher the impact of wetlands on these variations through the establishment of the riverine C budget. In the study, the estimated C fluxes are lateral hydrological inputs from land (i.e., from forest groundwater) and from wetlands to the river network, C degassing from the rivers and total C export to the ocean. The different C fluxes are estimated independently, allowing the quantitative determination of both C inputs from terrestrial ecosystems and from wetlands at the catchment scale. To the best of our knowledge, our study is the first to estimate lateral hydrological export of C both from wetland and from well-drained terrestrial ecosystem (i.e., from forest groundwater) in a tropical catchment. In lines with recent studies in tropical rivers (Abril et al., 2014; Borges et al., 2015; 2019), we expected that lateral inputs of C from wetlands to the river network are significant in comparison with C exported laterally from forest groundwater. We therefore hypothesized that the contribution of the net terrestrial C sink to the riverine carbon budget was minor.

2 Materials and Methods

2.1 Study site

The Nyong catchment (27800 km^2, Cameroon) is located between 2.8 and 4.5 ° N and 9.9 and 13.5 ° E in the Southern Cameroon Plateau (Fig. 1). The main stem (Nyong River, stream order 6) is 690 km long and flows into the Atlantic Ocean (Fig.1). The catchment lithology is mainly composed of granitic rocks with the absence of carbonate minerals (Maurizot et al., 1986; Toteu et al., 2001). Slopes and hills are recovered by a thick lateritic profile (20-40 m) poor in C, whereas in the depressions and the swamps the upper part of the hydromorphic soils shows an enrichment in organic matter (OM) (Boeglin et al., 2003; Nyeck et al., 1999). Most of the catchment area is covered by a dense permanent forest whereas semi-aquatic

https://doi.org/10.5194/bg-2021-69
Preprint. Discussion started: 7 April 2021

plants such as raffia or palm tress predominates in the swampy depressions. The Nyong catchment experiences an equatorial climate with four seasons of unequal importance with two maxima and minima: a short rainy season (Apr-June), a short dry season (July-August), a long rainy season (Sept.-Nov) and a long dry season (Dec-March) (Suchel, 1987). In 2016, the average annual precipitation in the basin measured in the Mengong catchment was ~1610 mm (Fig. 2). In 2016, the hydrological cycle, based on the hydrograph, can be separated into three four-months periods: base (Jan-Apr), medium (May-Aug) and high (Sep-Dec) flows (Fig. 2).

In the Nyong catchment, 6 sampling sites were selected: 2 located on the main stem (Mbalmayo and Olama) and 4 in the So'o sub-catchment (Mengong source, Mengong outlet, Awout and So 'o) (Fig. 1). The sampling sites cover a wide range of stream orders: from groundwater to order 6 (Table 1). Each sampling site (except the Mengong source) are equipped with gauging gauges calibrated for flow measurement, monitored daily since 1993 and are publically available at https://doi.org/10.6096/BVET.CMR.HYDRO. In 2016, the Nyong River flow at the most downstream station (Nyong at Olama) was 200 m^3 s^{-1} (Fig. 2) and export or riverine C at this site is considered as representative of the C epxorted to the Atlantic Ocean by the Nyong basin because the contribution of the tributaries downstream from this station is negligible (Nkoue-ndondo, 2008).

The Mengong catchment is considered representative of the tropical lateritic environments of the South Cameroon plateau (Braun et al., 2012). Therefore, hydro-biogeochemical processes occuring in the Mengong catchment are considered as representative of hydro-biogeochmical processes ocurring in the other first-order basins of the Nyong catchment. Noteworthy, at the Mengong source, groundwater seeps out from the hillside of the Mengong catchment and eventually converge to the stream (i.e., Mengong stream). Then, the Mengong flows donwstream trough a swamp located in the lowland part of the Mengong basin to eventually reach the Mengong outlet 850 m downstream of the seepage point (Maréchal et al., 2011). In the lowland part of the Mengong catchment, the Mengong stream is indeed adjacent to the swamp whose extent is on average through the year ~20% of the total surface area of the catchment (Braun et al., 2005). Accordingly, water at the Mengong outlet is fed by two different sources: the forest groundwater that seeps from the hillside of the Mengong catchment and by the swamp located in the lowland part of the basin (Maréchal et al., 2011). In the Mengong catchment, surface runoff on the slopes is negligible due to the high infiltration capacity of the soils and the relatively low slope (Maréchal et al., 2011). At the Nyong catchment scale, surface runoff is also of small magnitude and might not contribute significantly to the input of terrestrial C to surface waters (Nkoue-ndondo, 2008). The geographical and hydrological characteristics of the different sub-catchments are shown in Table 1.

2.2 Sampling and laboratory work

Water in the Nyong, So'o and Awout Rivers was collected from bridges with the Niskin Bottle (3L). At the Mengong source, samples were taken directly from the source where the groundwater seeps through an inert PVC pipe. At the Mengong outlet, because of the shallow depth, the samples were cautiously taken directly in the stream. Water samples were collected from January to December 2016 with a fortnightly frequency (22 times during the sampling period). We measured dissolved

https://doi.org/10.5194/bg-2021-69
Preprint. Discussion started: 7 April 2021

inorganic C (DIC), TA, dissolved organic (DOC) and particulate organic (POC) C and total suspended matter (TSM). At each samplig site, we measured the physico-chemical parameters of the water (temperature, pH, dissolved oxygen as O_2, and specific conductivity). In addition, we carried out 14 measurements of pelagic respiration at two sampling sites (Mengong outlet and Nyong at Mbalmayo, which are first- and fifth-order streams, respetively).

The water temperature, pH, dissolved oxygen and specific conductivity were measured *in situ* in 2015 and between January and March 2016 using portable probes (WTW®). Calibration of sensors was carried out prior to the sampling campaigns and regularly checked during the campaigns. The conductivity cell was calibrated with a 1000 µS cm $^{-1}$ (25°C) standard. The oxygen optical probe was calibrated with humidity saturated ambient air. The pH probe was calibrated using NBS buffer solutions (4 and 7). From April 2016, a multi-parameter probe (YSI ProDSS) was used for *in situ* measurements of the same physico-chemical parameters. The multi-parmater probe was calibrated before each sampling campaign using standard protocols (YSI Proplus).

For TSM and POC, a first filtration (0.5-1.5 L) was carried out on pre-weighed and pre-combusted GF/F glass fiber filters (porosity of 0.7 µm). The filters were dried at 60 °C and stored in the dark at room temperature for subsequent analysis. TSM was determined by gravimetry with a Sartorius scale (precision was ±0.1 mg). The filters were acidified in crucibles with 2N HCl to remove carbonates and were then dried at 60 °C to remove inorganic C and the remaining acid and water and then analyzed by the Rock Eval pyrolysis method (Lafargue et al., 1998). For DOC analysis, a portion of the POC filtrate was kept in glass bottles (60 mL) previously pyrolyzed in which 3 drops of H_3PO_4 (85%) were added to convert all the DIC into CO_2. The glass bottles were sealed with septas made of polytetrafluoroethylene (PTFE). The samples were stored at 3-5°C before analysis. DOC concentrations were measured by thermal oxidation after a DIC removal step with a SHIMADZU TOC 500 analyser in TOC-IC mode (Sharp, 1993). The repeatability was better than 0.1 mg L^{-1}.

We stored TA samples in polypropylene bottles after filtration using a syringe equipped acetate cellulose filters (porosity of 0.22 µm). TA was analyzed on filtered samples by automated electro-titration (Titrino Metrohm) on 50 mL-samples with 0.1N HCl as the titrant. The equivalence point was determined from pH between 4 and 3 with the Gran method (Gran, 1952).

The DIC samples were collected using 70 mL glass serum bottles sealed with a rubber stopper and treated with 0.3 mL of $HgCl_2$ at 20 g L^{-1} to avoid microbial respiration during storage. Vials were carefully sealed such that no air remained in contact with samples and were stored in the dark to prevent photo-oxidation. The DIC was measured with the headspace technique. The headspace was created with 15 mL of N_2 gas, and 100 µL of phosphoric acid (H_3PO_4, 85%) was added in the serum bottles in order to convert all the DIC species to CO_2. After overnight equilibration at constant temperature, a subsample of the headspace (1 mL) was injected with a gastight syringe into a gas chromatograph equipped with a flame ionization detector (SRI 8610C GC-FID). The gas chromatograph was calibrated with CO_2 standards of 400, 1000 and 3000 ppm (Air Liquide® France).

Six extra 70 mL serum bottles were collected similarly as DIC and then were used for the determination of pelagic respiration. Three serum bottles were directly poisoned in the field with 0.3 mL of $HgCl_2$. The three other serum bottles were incubated in a cool box during 24 hours. The cool box was protected from light and filled with water from the river to maintain inside the

https://doi.org/10.5194/bg-2021-69
Preprint. Discussion started: 7 April 2021

cool box a water temperature similar to the one in the river. At the end of the incubations, the serum bottles were poisoned with 0.3 mL of $HgCl_2$ and stored in the dark and at room temperature. To estimate pelagic respiration, we measured the increase in CO_2 in the incubated serum bottles compared to those poisoned in the field. CO_2 was measured similarly as DIC, using a headspace technique but without acidification.

In the surface waters of the Nyong catchment, we estimated the pCO_2 from DIC, pH and water temperature measurements using the carbonic acid dissociation constants of Millero (1979) and the CO_2 solubility from Weiss (1974); using the CO_2SYS software (Lewis et al., 1998).

2.3 Determination of catchments surface area, water surface area, slope and gas transfer velocity (k_{600})

The sub-catchments surface areas were estimated from hydrological modeling tools available in ArcGIS10.5® and the digital elevation model (DEM, 15 sec resolution) conditioned for hydrology (HydroSHEDS; Lehner et al., 2008). Wetlands surface areas were estimated from Gumbricht et al. (2017). In the Nyong catchment, the HydroSHEDS flowline dataset (15 sec resolution) enabled the precise determination of the total length of each stream order (1 to 6). We combined the river flow measurements from the five gauging stations located on stream-orders 1, 3, 4, 5 and 6 (Table 1) and the hydraulic equation described by Raymond et al. (2012) in order to estimate the average river width (W) for all rivers of a given stream orders:

$$W = 12.88 Q_{mean}^{0.42}$$

where Q_{mean} is the mean river flow in 2016 in the stream orders 1, 3, 4, 5 or 6.

Within a basin, river length, width, and surface area scale exponentially with stream order for all river orders (Strahler, 1957). Since we did not measure river flow in stream order 2, the average width of stream order 2 was extrapolated from the best exponential regression curve obtained from the relationship between stream order and average river width in the catchment. We then used the average river width (estimated from hydraulic equation by Raymond et al. 2012) and the total length per stream order (estimated from HydroSHEDS flowline dataset) to calculate the water surface area per stream order. We fused the HydroSHEDS DEM and flowline datasets to assign an altitude to each river point and thus to determine the average slope (S) per stream order. To calculate the average flow velocity (V) per stream order, we used the following hydraulic equation:

$$V = 0.19 Q_{mean}^{0.29}$$

where Q_{mean} is the mean river flow in 2016 in the stream orders 1, 3, 4, 5 or 6. The average flow velocity in stream order 2 was extrapolated similarly as the the average river width (see above). The gas transfer velocity normalized to a Schmidt number of 600 (k_{600} in m d^{-1}) was derived from the parameterization as a function of S (unitless) and V (m s^{-1}) as in the Eq. 5 by Raymond et al. (2012):

$$k_{600} = VS*2841+2.02$$

As described by Borges et al. (2019), we chose this parameterization because it is based on the most comprehensive compilation of k values in streams which, in addition, was used in the global upscaling of CO_2 emissions from rivers by both Raymond et al. (2013) and Lauerwald et al. (2015).

https://doi.org/10.5194/bg-2021-69
Preprint. Discussion started: 7 April 2021

2.4 C fluxes estimation

2.4.1 C degassing

The CO_2 degassing at the water-air interface (F_{degas}) was estimated as follows:

$$F_{degas} = k_{600} K_0 (p_{CO2w} - p_{CO2a})$$

where K_0 is the solubility coefficient of CO_2 determined from the water temperature (Weiss, 1974), k_{600} is the gas transfer velocity of CO_2 (see section 2.4), pCO_{2w} and pCO_{2a} are the partial pressures of CO_2 in the surface water and in the overlying atmosphere (set to 400 ppmv), respectively.

We estimated F_{degas} (mmol m^{-2} d^{-1}) in each stream order of the Nyong basin (1 to 6) and we multiplied F_{degas} by the respective surface area of each stream order to estimate the total CO_2 emission (Gg C yr^{-1}) per stream order. We summed the total CO_2 emission in each stream order to estimate the total quantity of CO_2 degassed in the basin by the entire river network. We normalized the latter flux by the surface area of the Nyong catchment to estimate an average degassing weighed by the surface area of the basin (t C km^{-2} yr^{-1}). Note that we did not measured pCO_2 in second-order streams. However, we estimated the average pCO_2 in second order streams by averaging the pCO_2s observed in the first and third order streams.

2.4.2 Lateral inputs of C from land and wetland

In the Nyong basin, we considered that lateral inputs of C in the river network originates from two sources: forest groundwater (i.e., terrestrial C) and wetlands (i.e., semi-aquatic C). In our study, these two lateral inputs were estimated from data acquired in the Mengong catchment. Maréchal et al. (2011) estimated that the recharge rate of the hillside of the Mengong catchment was 332 mm yr^{-1} (between 1994-1998). The recharge rate of the hillside comprises two hydrological fluxes: one is hillside groundwater outflow and one is baseflow from the hillside to the swamp (Maréchal et al. 2011). The hillside drains a surface area of 0.48 km^2, thereby the average annual outflow of the terrestrial groundwater (Q_{GW}) is ~0.005 m^3 s^{-1}, from which an hydrological lateral export of C from forest groundwater to surface waters (F_{GW}) can be estimated as the following:

$$F_{GW} = Q_{GW} [C]_{GW}$$

where $[C]_{GWr}$ is the average annual concentration of DIC or DOC in the Mengong source. Fex_{GW} (t C yr^{-1}) is normalized by the surface area drained by the hillside (t C km^{-2} yr^{-1}).

In the Mengong catchment, Maréchal et al. (2011) estimated that the swamp flows to the stream at an average rate of 589 mm yr^{-1} and the swamp drains an average surface area of 0.12 km^2, thereby the average annual outflow of the swamp (Q_{SW}) is ~0.002 m^3 s^{-1}. Hydrological lateral export of semi-aquatic C ($F_{SW_{DIC,DOC}}$) from the swamp (wetland domain) to surface waters can thus be estimated as the following:

$$F_{SW_{DIC,DOC}} = Q_{SW} [C]_{SW}$$

where $[C]_{SW}$ is the average annual concentration of DIC or DOC in the swamp of the Mengong catchment. $F_{SW_{DIC,DOC}}$ (t C yr^{-1}) is normalized by the surface area drained by the swamp (t C km^{-2} an^{-1}). DOC and DIC concentrations in the swamp were estimated from DIC and DOC measured by Nkoue-ndondo et al. (2020) in the soil solution of the swamp at 0.4 meter depth.

https://doi.org/10.5194/bg-2021-69
Preprint. Discussion started: 7 April 2021

In the Mengong catchment, surface runoff is negligigble and there is no particulate C in forest groundwater, therefore, the POC at the Mengong outlet should originates mostly from the drainage of the swamp (which is adjacent to the stream). Accordingly, we considered the lateral hydrological export of POC at the outlet of the Mengong catchment (i.e., Mengong outlet) representative of the POC exported laterally from the swamp (F_{SWPOC}). F_{SWPOC} can be thus estimated as the following:

$$F_{SWPOC} = Q_{outlet}\,[POC]_{outlet}$$

where Q_{outlet} is the average annual river flow at the Mengong outlet and $[POC]_{outlet}$ is the average annual concentration of POC at the Mengong outlet. F_{SWPOC} (t C yr^{-1}) is normalized by the surface area drained by the swamp (t C km^{-2} an^{-1}).

2.4.3 Internal metabolism in the river network

F_{respi} (mmol m^{-3} d^{-1}) is the average pelagic respiration obtained from the increase in CO_2 in the incubated serum bottles over 24h. F_{respi} was converted in mmol m^{-2} d^{-1} by multiplying by the average river depth at the corresponding sampling site. Noteworthy, F_{respi} does not represent total respiration in the river since it does not include benthic respiration. A mean benthic respiration measured in various tropical rivers of 21 mmol m^{-2} d^{-1} (Cardoso et al., 2014) was therefore added to estimate total F_{respi} which is used throughout the manuscript.

2.4.4 C export to the ocean

The annual average C exported to the ocean (F_{ocean}) was calculated at Olama as the following:

$$F_{ocean} = Q_{olama}\,[C]_{olama}$$

where Q_{olama} and $[C]_{olama}$ are the annual average flow and concentrations of POC, DIC or DOC at Olama, respectively. F_{ocean} was estimated in Gg C yr^{-1} and then normalized by the catchment surface area at Olama (t C km^{-2} $year^{-1}$).

2.5 C budget in the waters of Nyong basin

The sum of the C transferred by forest groundwater (F_{GW}) and by wetland (F_{sw}) represents the total C inputs (C_{inputs}) transferred laterally to the river network, thus:

$$C_{inputs} = F_{SW\,(DOC,\,DIC,\,POC)} + F_{GW\,(DOC,\,DIC)}$$

The C entering the surface network has two outputs ($C_{outputs}$) as this C is degassed at the water-air interafce (F_{degas}) or exported to the ocean (F_{ocean}), thus:

$$C_{outputs} = F_{ocean\,(DOC,\,DIC,\,POC)} + F_{degas}$$

The difference between C_{inputs} and $C_{outputs}$ represents the C budget (C_{budget}) in inland waters of the Nyong basin, as the following:

$$C_{budget} = C_{inputs} - C_{outputs}$$

Noteworthy, external C_{inputs} assumed to be provided by both forest groundwater and wetland should sustain total F_{respi}. Therefore, total F_{respi} is not included in the estimation of C_{budget}.

https://doi.org/10.5194/bg-2021-69
Preprint. Discussion started: 7 April 2021

2.6 Statistical procedures

To assess statistical differences between stream orders (upstream-downstream) or between seasons (related to base, medium and high flows), we used the ordinary one way-ANOVA with Tukey's multiple comparisons test for data normally distributed whereas we used Kruskall-Wallis test with Dunn's multiple comparison test for data that were not normally distributed. For both statistical tests, $p>0.05$ indicated that samples did not differ significantly, while $p<0.05$ indicated a statistical difference and $p<0.001$ an even higher confidence level of statistical difference. To assess correlations between a given parameter and river flow we used a Pearson correlation test for data normally distributed and Spearman correlation test for data that were not normally distributed. For these correlation tests, $p>0.05$ indicated that samples were samples were not correlated, while $p<0.05$ indicated a correlation and $p<0.001$ an even higher confidence level of correlation. Normality was tested with the Agostino & Pearson normality test. All tests were made with Golden Software Prism (version 7).

3 Results

3.1 Seasonal and spatial variations of physico-chemical parameters

In forest groundwater and surface waters of the Nyong Basin, water temperature ranged between 21.9 and 29.0 °C, pH between 4.6 and 6.8, O_2 between 12 and 81% and specific conductivity between 5.1 and 86.3 µS cm^{-1} (Table 2; Fig. 3). Minimum values of water temperature and specific conductivity were observed in the Mengong outlet (21.9 °C and 13.1 µS cm^{-1}, respectively, stream order 1) whereas maximum values were observed in the Nyong River at Mbalmayo (29.0 °C and 86.3 µS cm^{-1}, stream order 5) (Table 2; Fig. 3). For oxygen saturation, both minimum and maximum values were observed in the Nyong River at Mbalmayo (13-81%) (Table 2; Fig. 3). For pH, minimum values were observed in the Mengong source (4.6, groundwater) whereas maximum values were observed in the Nyong River at Mbalmayo (6.9) (Table 2; Fig. 3).

Spatially, on average throughout the year, water temperature, pH and specific conductivity increase from upstream (i.e., groundwater) to downstream (i.e., order 6) (Table 2; Fig. 3). Along an upstream-downstream gradient, annual-averaged oxygen saturation peaked significantly ($p<0.001$) in the So'o River (57%, order 4) (Table 2; Fig. 3). In the groundwater and stream orders 1, 3 ,5 and 6 oxygen saturations were significantly lower than in the So'o River but similar ($p>0.05$) between each other's (Table 2; Fig. 3). In general, temporal variation are related to river flows pH, oxygen saturation and specific conductivity were inversely related to the river flow in the groundwater and all stream orders (Fig. 3). During base flow conditions, values of water temperature increased significantly ($p<0.05$) in forest groundwater and most of the stream orders (Fig. 3). Specific conductivity was also significantly higher ($p<0.05$) during base flow conditions in all stream orders, except in groundwater (Fig. 3).

https://doi.org/10.5194/bg-2021-69
Preprint. Discussion started: 7 April 2021

3.2 Seasonal and spatial variations of particulate compounds (i.e., TSM, POC% and POC)

In surface waters of the Nyong Basin, TSM ranged between 1.8 and 27.5 mg L^{-1}, POC content in the TSM (i.e., POC%) between 9 and 29% and POC between 14 and 360 µmol L^{-1} (Tables 2-3; Fig. 4). On average throughout the year, TSM was significantly ($p<0.05$) lower in in the Mengong outlet (stream order 1) than in stream orders 3, 4, 5 and 6 (Table 2; Fig. 4). POC% was significantly ($p<0.05$) higher in stream order 1 than in stream orders 3, 4, 5 and 6 (Table 3; Fig. 4). In general, on average throughout the year, we observed from upstream (stream order 1) to downstream (stream order 6) an increase in TSM and a concomitant decrease in POC% (Tables 2-3; Fig. 4). In contrast, on average throughout the year, POC was similar ($p>0.05$) within all stream orders (Table 3; Fig. 4). Irrespective of the stream orders, TSM, POC% and POC were in general higher (sometimes significantly) during medium and high flows than base flow (Fig. 4). Besides, when all data are plotted together, TSM and POC are both strongly correlated ($p<0.001$) with river flow (data not shown).

3.3 Seasonal and spatial variations of dissolved compounds (i.e., pCO_2, TA, DIC and DOC)

The surface waters of the Nyong Basin were low-buffered (TA: 10-265 µmol L^{-1}), highly oversaturated in CO_2 in comparison to the overlying atmosphere (pCO_2: 3000-41000 ppmv) and organic-rich (DOC: 1,020-7,550 µmol L^{-1}) (Table 3; Fig. 5). Forest groundwater was also low-buffered (TA: 15-138 µmol L^{-1}) and highly oversaturated by CO_2 in comparison to the overlying atmosphere (pCO_2: 12700-209000 ppmv but exhibited very low DOC concentrations (108±10 µmol L^{-1}) (Table 3; Fig. 5). On average throughout the year, pCO_2 generally decreased along the upstream-downstream gradient, but particularly between the Mengong source and its outlet, which is located 850 m downstream the source (Table 3; Fig. 5). Water at the Mengong outlet exhibited a pCO_2 ~four times lower than at the Mengong source (Table 3; Fig. 5). In the Mengong source, DIC was mostly in the dissolved CO_2 form (~97%), TA representing ~3%, contrasting with surface waters where TA represented on average 26% of the DIC (Table 3). In forest groundwater and stream orders 1, 3 and 4, TA did not differ significantly ($p>0.05$) but TA increased significantly ($p<0.001$) in the main course of the Nyong River (stream order 5 and 6) (Table 3; Fig. 5). On average throughout the year, DOC concentration in surface waters did not exhibit variations in relation with stream order. However, DOC in the Awout River (order 3) peaked significantly ($p<0.001$) in comparison with other stream orders (Table 5; Fig. 5). Seasonally, TA was inversely related ($p<0.001$) with the river flow in each stream order (data not shown), except in the groundwater where TA was constant ($p>0.05$) throughout the year (Fig. 5). The coefficient of variation of pCO_2 was 48% (Mengong source), 42% (Mengong outlet), 56% (Awout), 58% (So'o), 55% (Nyong at Mbalamayo) and 60% (Nyong at Olama), which indicated a strong temporal variability of pCO_2 in the groundwater and surface waters of the Nyong basin (Table. 2). Indeed, in the groundwater and surface waters, pCO_2 was generally higher (but not significantly) during medium and high flow conditions than during base flow (Fig. 5). However, in the stream orders 4, 5 and 6, pCO_2 is positively correlated ($p<0.05$) with river flow (data not shown). In stream order 1, DOC peaked significantly ($p<0.05$) during base flow conditions whereas in stream orders 3, 4, 5 and 6, DOC was similar ($p>0.05$) for all seasons (Fig. 5).

https://doi.org/10.5194/bg-2021-69
Preprint. Discussion started: 7 April 2021

3.4 Carbon mass balance of the Nyong River

At the basin scale, 12.1±5.8 and 15.5±7.2 t C km^{-2} yr^{-1} are drained by forest groundwater and wetlands, respectively (Fig. 6). POC, DOC and DIC represents 5, 30 and 65%, respectively, of the C exported laterally to surface waters by wetlands (Fig. 6). DOC and DIC represents 3 and 97%, respectively, of the C exported laterally to surface waters by forest groundwater (Fig. 6). At the most downstream station, 7.2±0.5 t C km^{-2} yr^{-1} are exported to the Atlantic Ocean, in which 25, 69 and 6% are in the DIC, DOC and POC forms, respectively (Fig. 6). Total inputs from wetlands and terrestrial ecosystems and total outputs (emissions to the atmosphere and export to the ocean) are fairly balanced as the difference between $C_{outputs}$ and C_{inputs} was 16%, and $C_{outputs}$ and C_{inputs} were not statistically different from each other's. Given the high temporal variability in streams and rivers, this shows that our methodology was fairly robust.

4 Discussion

4.1 Dynamics and origin of C in forest groundwater

Considering the granitic lithology (i.e., absence of carbonate minerals) of the Nyong basin (Maurizot et al., 1986), TA in forest groundwater originates from the weathering of silicate minerals as dissolved CO_2 can react with silicate minerals to produce bicarbonates (Meybeck, 1987). In forest groundwater, the low TA concentrations and the absence of significant seasonal variations of TA were likely related to low weathering rates in the lateritic soil cover, which exhibits a relatively inert mineralogy (Braun et al., 2005, 2012). Based on TA concentrations (53±26 µmol L^{-1}) in forest groundwater and seepage of the groundwater of ~0.005 m^3 s^{-1}, we estimated a weathering rate in forest groundwater and overlaying lateritic soil of 0.2±0.1 t C km^{-2} yr^{-1}. The low weathering rates are mainly attributed to the thickness of the lateritic cover on hills and slopes, which considerably slows the advance of percolating water in the bedrock (Boeglin et al., 2005). This was confirmed by the low mineral dissolved load in the aquifer of the Nyong basin (Braun et al., 2002) and by the dissolved silica fluxes in rivers that were significantly lower compared to the annual rainfall (e.g., White and Blum, 1995). Accordingly, in the Nyong basin, forest groundwater is therefore a limited source of TA for surface waters, as reported in other monolithic catchments draining only silicate rocks (Meybeck, 1987).

The dissolved CO_2 in groundwater originates from the solubilization of soil CO_2 that originates itself either from soil OM respiration in the unsaturated soil (Raich and Schlesinger, 1992), in the saturated soil or in the groundwater itself, using DOC that has been leached from the soil (Deirmendjian et al., 2018). In the Mengong source, groundwater pCO_2 and O_2 were not correlated ($p>0.05$, data not shown) and groundwater was free of DOC (Table 2; Braun et al., 2012; Brunet et al., 2009). In the lateritic soil overlaying the Mengong source, iron oxides represent up to 50% of the average volumetric weight of the soil (Braun et al., 2005). Thus, the low concentrations of dissolved iron (Fe^{2+}) observed in the Mengong source indicated that despite the oxidizing environment above the groundwater, the transfer of Fe^{2+} from the soil to the aquifer is not allowed (Braun et al., 2005). OM in the upper organic-rich horizons of the soil is probably well complexed with iron oxides and prevents DOC

https://doi.org/10.5194/bg-2021-69
Preprint. Discussion started: 7 April 2021

leaching to groundwater (Deirmendjian et al., 2018; Sauer et al., 2007). Based on this information, we hypothesize that groundwater pCO_2 did not originate from respiration in the groundwater itself but originated mainly from soil respiration occurring in the overlaying unsaturated soil (Fig. 6). On average throughout the year, groundwater pCO_2 was ~50 times higher than the atmospheric value showing that forest groundwater is a major source of CO_2 for the river network of the Nyong basin (Table 3).

In tropical forests, seasonal variations of soil temperature are relatively low throughout the year, and therefore, the soil water content is the main parameter controlling the intensity of soil respiration (Adachi et al., 2006; Hashimoto et al., 2004). During base flow, precipitation was low compared to the two other hydrological periods (Fig. 2), likely decreasing soil moisture and thus soil respiration.. During the following periods of medium and high flows, precipitation increased (Fig. 2), which in turn had likely a positive effect on soil respiration. In addition, during medium and high flows periods the groundwater level has risen closer to surface organic-rich horizons where soil respiration is more intense (Amundson et al., 1998; Maréchal et al., 2011). During high flow conditions, the percolation of rainwater through the soil pores may also facilitated the transport and the dissolution of soil CO_2 to the underlying groundwater. Altogether, this may explain the lower groundwater pCO_2 and the higher groundwater O_2 observed during base flow conditions (Figs. 3, 5).

4.2 Dynamics and origins of C in the Mengong catchment (first-order stream)

There are two main types of waters in the Mengong catchment (and in the Nyong catchment): clear waters and colored waters (Boeglin et al., 2005). Clear waters exhibited very low DOC concentrations (<0.1 mg L^{-1}) and come from springs (i.e., forest groundwater) that seeps out from hills and slopes, whereas colored waters, constituting the river waters, exhibited higher DOC concentrations (>14 mg L^{-1}) and originated from surface waters located in depressions (i.e., from swamp located in the lowland part of the catchment) (Boeglin et al., 2005; Ndam Ngoupayou, 1997). When clear waters flow through swamps, the chemistry of clear waters is significantly affected downstream. Accordingly, significant increases in DOC and POC concentrations were observed between the Mengong source (i.e., clear water) and its outlet (i.e., colored water) because the Mengong stream has flowed through the swamp which occupies 20% of the surface of the basin (Table 2). The Mengong source is free of both DOC and POC (i.e., below the detection limit) and is oxygenated throughout the year (Table 2). Therefore, POC and DOC at the Mengong outlet originates almost exclusively from the drainage and erosion of the swamp, as observed by Nkoue-Ndondo et al. (2020) based on the stable isotopic composition of DOC and POC in the Mengong basin. Tropical wetlands such as swamps are recognized as productivity hotspots (Borges et al., 2015b; Saunois et al., 2019) and a large fraction (excluding wood) of their biomass is degraded *in situ* by heterotrophic respiration in the water and sediment which enrich swamp water in CO_2 (Fig. 6; Abril and Borges, 2019). High biological productivity in wetlands also explains significantly higher POC% observed in the Mengong outlet in comparison with the other stream orders, which exhibited lower wetland surface area in their basin, diluting POC% (Table 3; Fig. 4). In addition, wetland vegetation can actively transport oxygen to the root zone via their aeremchyma (Haase and Rätsch, 2010). This creates a complex oxic-anoxic interface that promotes aerobic respiration, but also supplies labile OM to anaerobic degradation and methanogenesis fuelling CO_2 and CH_4 production and other fermentative

https://doi.org/10.5194/bg-2021-69
Preprint. Discussion started: 7 April 2021

organic compounds that are transferred to waters and pore waters (Piedade et al., 2010). Nkoue-Ndondo et al. (2020) measured on average through the year, high concentrations of DIC and DOC in the swamp of the Mengong catchment in the range of 150-3270 and 140-1510 µmol L^{-1} for DIC and DOC, respectively. Noteworthy, we observed significant higher DOC concentrations during base flow at the Mengong outlet (Fig. 5), which might be explained by longer water residence time in the swamp during this period.

In comparison to the Mengong source, TA concentrations significantly increased (~two times) in the Mengong outlet after the stream has flowed through the swamp (Table 3; Fig. 5). In addition, based on TA concentrations (90±36 µmol L^{-1}) and average river flow at the Mengong outlet, we estimated a weathering rate of 0.5±0.2 t C km^{-2} yr^{-1}, which is 150% higher than weathering rate in forest groundwater. This weathering rate was comparable to the previous estimate by Boeglin et al. (2005) for the entire Nyong catchment of 0.8-1.1 t C km^{-2} yr^{-1}, but was three times lower than those previously estimated for other lateritic basins (see Boeglin et al., 2005). This indicates that swamps in the Nyong river basin are a limited but significant source of TA for surface waters of the watershed. Under reducing conditions usually occurring in swamps, ferro-reducing bacteria can use iron oxides to oxidized OM and this process produces TA (ΔTA = + 2.2 moles of TA produced for 1 mole of iron oxide consumed; Abril and Frankignoulle, 2001). The contribution of Fe(III) reduction to anaerobic carbon metabolism in a given environment is mainly proportional to the availability of labile OM and reducible Fe(III) (Roden and Wetzel, 2002). In the Mengong catchment, these two substrates are abundant in the hydromorphic soils of the swamp (Braun et al., 2005). In the swamp of the Mengong basin, Braun et al. (2005) observed a vertical decrease in Fe(III) in the soil profiles, confirming that the swamp behaves as hotspot of Fe(III) reduction and TA production (Liesack et al., 2000). In addition, weathering rates in the swamp area of the Mengong catchment is enhanced by the leaching of humic acids from the vegetation to the hydromorphic soils (Braun et al., 2005; Nkoue-Ndondo, 2008).

4.3 C variations at the scale of the Nyong catchment

At the scale of the Nyong basin, TA increased along an upstream-downstream gradient and TA was inversely related with river flow (Fig. 5). During base flow period, surface waters are fed by deeper groundwater level, which are older and likely exhibited higher TA concentrations than shallower levels. In addition, we suppose that during high flow TA is diluted by forest groundwater and swamp waters with lower TA concentrations.

In contrast to temperate rivers, the pCO_2 in the surface waters of the Nyong basin peaked during periods of high waters (Fig. 5). This seasonality can be explained by the fact that soil moisture increases during the rainy season, enhancing the respiration in the soil surface organic-rich horizon. Concomitantly, period of high waters probably increases the hydraulic gradient between forest groundwater and surface waters, increasing the flushing of forest groundwater when groundwater pCO_2 is the highest (Fig. 5). In addition, the rise of the water level in the watershed enhances of the connection of surface waters with wetlands during periods of high waters. Therefore, the CO_2 resulting from the degradation of the wetland biomass can be transferred to the river main stem. These two processes explain why usually pCO_2 is positively correlated with river flow in tropical rivers, (e.g., Borges et al., 2019; Bouillon et al., 2012).

https://doi.org/10.5194/bg-2021-69
Preprint. Discussion started: 7 April 2021

In the surface waters of the Nyong catchment, the supersaturation in CO_2 in comparison to the overlying atmosphere and the decrease of pCO_2 from groundwater to stream order 6 showed a gradual degassing of CO_2 at the water-air interface along an upstream-downstream gradient (Table 3; Fig. 5). In acidic waters, CO_2 degassing at the water-air interface is related with an the increase of the $\delta^{13}C$ of the DIC (Deirmendjian and Abril, 2018). Such a pattern was observed by Brunet et al. (2009) in the waters of the Nyong basin confirming the upstream-downstream degassing. It confirms that headwaters are a major source of CO_2 for the river system. Groundwaters are obviously a significant source of CO_2 for the headwaters. However, in tropical rivers like the Nyong which do not have floodplains, most of the wetlands are actually located in low order streams and therefore fuels small tributaries with CO_2 which is mostly degassed further downstream in the main stem.

We also observed an increase in POC, in the surface waters during periods of high waters, concomitant to the increase in pCO_2 (Figs. 4-5). Similarly to what we observed in the Mengong catchment, wetlands can also be considered as the main source of POC for surface waters in the entire Nyong basin based on (1) the low slopes in the catchment, (2) the high infiltration capacity of the soil and (3) the probable low pelagic primary production in the surface waters. During the high-water stage, dissolved and particulate C from wetlands are flushed to surface waters, as frequently observed in tropical catchments and confirmed by the increase in POC% in stream orders 4, 5 and 6 during periods of high water stages (Fig. 5) which reflect the high biological productivity of these ecosystems. Indeed, wetlands exhibited higher POC% compared to rivers, as indicated by the highest values of POC% observed in the Mengong outlet, the latter being strongly influenced by wetland (Fig. 5). In addition, the normalized export of POC from wetland to rivers and from the watershed to the ocean is similar (Fig. 6). This confirms that wetlands are the main source of POC for surface waters, in particular during periods of high waters, and that degradation of POC in the riverine water is not significant. At the scale of the Nyong basin, the increase in connectivity between wetlands and surface waters during periods of high waters is also in agreement with a significant drop in O_2 saturation during these periods because the flooding of OM-rich wetlands enhance respiration (Fig. 3). We also observed a remobilization of mineral matter from the riverbanks and beds during high waters periods, as evidenced by higher TSM in the Nyong River during these hydrological periods (Fig. 4). When all data are plotted, POC% and TSM were negatively correlated together ($p<0.001$), showing a dilution of the POC with mineral matter from upstream to downstream.

In surface waters, by contrast to pCO_2 and POC, we did not observe a positive correlation between DOC and the river flow, in agreement with Brunet et al. (2009) who showed that DOC was only flushed during a short period of time at the beginning of the rainy season (in September and in April). In the Awout River (order 3), a significant increase in DOC was observed during medium flow period indicating an additional source of DOC (Table 2; Fig. 4). The Awout River was dry during the previous base flow period: its riverbed was completely invested by large macrophytes (up to 2 m tall) and many small pockets of stagnating water remained (visual observations). During base flow period, DOC could accumulate in these stagnating waters and then it is remobilized when the water flows again, as observed in temperate rivers (Deirmendjian et al., 2019; Sanders et al., 2007). As we do not see a general increase of DOC in base flow period in the whole watershed we believe that these local vegetation regrowth in river beds and riverbanks have a minor impact of the whole carbon balance in the Nyong watershed.

https://doi.org/10.5194/bg-2021-69
Preprint. Discussion started: 7 April 2021

4.4 C budget in the Nyong basin

We measured each fluxes of the riverine C budget independently and we show that 60% of the carbon entering the riverine system originates from wetlands, which makes them the main source of C in the river, the remaining 40% being transferred by forest groundwater. Therefore, our results are in lines with the growing consensus that tropical wetlands contribute significantly to the riverine C budget in the tropics. (Abril and Borges 2019; Abril et al., 2014; Borges et al., 2015a-b,)

A major portion (~80%) of the C entering surface waters returns to the atmosphere trough degassing at the water-air interface. In the Nyong catchment, *in situ* respiration (pelagic plus benthic) was on average 89 mmol m^{-2} d^{-1} whereas the average degassing was 1260 mmol m^{-2} d^{-1} (Table. 4), which implies that only ~7% of the degassing at the water-air interface was supported by *in situ* respiration. This is coherent with previous observations by Borges et al. (2015a) and (2019) in 12 African watersheds. Accordingly, our observations and measurements in the Nyong basin suggest the same conclusion: net heterotrophy in the river *sensu stricto* plays a minor role in the riverine CO_2 budget. Therefore, we can hypothesize that most of the CO_2 emitted by the rivers is actually produced in the wetlands and soils/groundwater and transferred to rivers where it escapes to the atmosphere.

In the Nyong catchment, the ratio between the C exported to the ocean and emitted to the atmosphere is 1:0.3, in agreement with ratio 1:0.2 measured by Borges et al., (2015a) in the Congo river but contrasting with the global ratio of 1:1 estimated by Ciais et al. (2013) during the Fifth Assessment Report of the Intergovernmental Panel on Climate Change (IPCC). It shows that at least African Rivers but probably all tropical rivers are strong emitters of C and therefore biogeochemical data in these rivers are urgently required to improve accuracy of regional and global C emission estimates from inland waters, and understand how they will respond to climate change (warming, change in hydrological cycle).

The integration of these fluxes at the scale of the whole watershed can be done by comparing this carbon budget with the terrestrial carbon budget. Brunet et al. (2009) estimated the net terrestrial C sink of the mature forest of the Nyong basin at approximately 300 t C km^{-2} yr^{-1}. Thus, the hydrological export of terrestrial C (via forest groundwater) represents ~4% of the terrestrial C sink. This conclusion is in agreement with the two local studies in temperate rivers, which have shown that the hydrological export of C from forest ecosystems is ~3% (Deirmendjian et al., 2018b; Kindler et al., 2011). Altogether, this study not only confirms the importance of the C inputs from wetlands for fuelling the riverine C cycle and most importantly CO_2 emissions to the atmosphere but it shows that high emissions from inland waters are compatible with a strong terrestrial C sink.

Conclusions

The current paradigm to explain CO_2 emissions from inland waters is based on the prevalence of heterotrophy sustained by terrestrial OM inputs from the terrestrial ecosystems to the aquatic systems. However, in the present study, we showed that degassing of riverine C at the water-air interface cannot be supported by river heterotrophy, as river heterotrophy represents

https://doi.org/10.5194/bg-2021-69
Preprint. Discussion started: 7 April 2021

480 ~7% of the average degassing. Thus, we highlighted the importance of lateral inputs of C from soils and groundwater on the one side (40% of the total C inputs), and from wetlands (60%) on the other side, to understand C dynamics in tropical rivers. Terrestrial groundwater was a significant source of C for surface waters, particularly for CO_2, whereas in contrast, DOC and POC in surface waters were mainly provided by the drainage and erosion of wetlands. The C exported laterally from wetlands to surface waters occurs mainly during periods of high waters when the connectivity with surface waters is enhanced. We
485 showed here by determining all the terms of the carbon mass balance independently that attributing the whole amount of carbon emitted to the atmosphere and exported to the ocean to a terrestrial source and ignoring the river–wetland connectivity can lead to the misrepresentation of C dynamics in tropical watersheds.

5 Acknowledgments

The Nyong Watershed is included in the CZO Multiscale TROPIcal CatchmentS (M-TROPICS, https://mtropics.obs-mip.fr),
490 LMI PICASS-EAU (https://picass-eau.ird.fr), LMI DYCOFAC (https://lab.ird.fr/collaboration/37/show) and OZCAR (Critical Zone Observatories: Research and Application) funded by IRD (Research Institute for Development—Institut de Recherche sur le Développement) and INSU/CNRS. We thank our colleagues from IRGM (Yaoundé, Cameroon) involved in M-TROPICS for their help in the field and in the laboratory. M. M. was funded by the French Embassy in Cameroon (Mobility Fellowship) and L. D. by IRD (Post-Doctoral fellowship). This research was supported by IRD and by Strategic planning
495 "PSIP Seq2C" (Interdisciplinary and Partnership Structuring Program on Continental Carbon Sequestration.

References

Abril, G. and Borges, A. V: Carbon leaks from flooded land : do we need to re-plumb the inland water Ideas and perspectives : Carbon leaks from flooded land : do we need to replumb the inland water active pipe ?, Biogeoscience, 16, 769–784, doi:10.5194/bg-16-769-2019, 2019.

500 Abril, G. and Frankignoulle, M.: Nitrogen-alkalinity interactions in the highly polluted scheldt basin (Belgium), Water Res., 35(3), 844–850, doi:10.1016/S0043-1354(00)00310-9, 2001.

Abril, G., Bouillon, S., Darchambeau, F., Teodoru, C. R., Marwick, T. R., Tamooh, F., Ochieng Omengo, F., Geeraert, N., Deirmendjian, L., Polsenaere, P. and Borges, A. V.: Technical note: Large overestimation of pCO<inf>2</inf>calculated from pH and alkalinity in acidic, organic-rich freshwaters, Biogeosciences, 12(1), 67–78, doi:10.5194/bg-12-67-2015, 2015.

505 Adachi, M., Bekku, Y. S., Rashidah, W., Okuda, T. and Koizumi, H.: Differences in soil respiration between different tropical ecosystems, Appl. soil Ecol., 34(2–3), 258–265, 2006.

Allen, G. H. and Pavelsky, T. M.: Global extent of rivers and streams, Science (80-.)., 361(6402), 585–588, doi:10.1126/science.aat0636, 2018.

Amundson, R., Stern, L., Baisden, T. and Wang, Y.: The isotopic composition of soil and soil-respired CO 2, Geoderma, 82(1–

510 3), 83–114, 1998.

Boeglin, J.-L., Ndam, J.-R. and Braun, J.-J.: Composition of the different reservoir waters in a tropical humid area: example of the Nsimi catchment (Southern Cameroon), J. African Earth Sci., 37(1–2), 103–110, 2003.

Boeglin, J., Probst, J., Ndam-Ngoupayou, J., Nyeck, B., Etcheber, H., Mortatti, J. and Braun, J.: Soil carbon stock and river carbon fluxes in humid tropical environments: the Nyong river basin (south Cameroon), in Soil Erosion and Carbon Dynamics,
515 Adv. Soil Sci, pp. 275–288, CRC Press Boca Raton, Fla., 2005.

Borges, A. V., Darchambeau, F., Lambert, T. and Morana, C.: Variations of dissolved greenhouse gases (CO2 , CH4 , N2O) in the Congo River network overwhelmingly driven by fluvial-wetland connectivity, Biogeosciences, 16(19), 3801–3834, doi:10.5194/bg-2019-68, 2019.

Borges, A. V, Darchambeau, F., Teodoru, C. R., Marwick, T. R., Tamooh, F., Geeraert, N., Omengo, F. O., Guérin, F.,
520 Lambert, T., Morana, C., Okuku, E. and Bouillon, S.: Globally significant greenhouse-gas emissions from African inland waters, Nat. Geosci., 8(8), 637–642, doi:10.1038/NGEO2486, 2015.

Bouillon, S., Yambélé, A., Spencer, R. G. M., Gillikin, D. P., Hernes, P. J., Six, J., Merckx, R. and Borges, A. V: Organic matter sources, fluxes and greenhouse gas exchange in the Oubangui River (Congo River basin), Biogeosciences, 9(6), 2045–2062, 2012.

525 Braun, J.-J., Dupré, B., Viers, J., Ngoupayou, J. R. N., Bedimo, J.-P. B., Sigha-Nkamdjou, L., Freydier, R., Robain, H., Nyeck, B. and Bodin, J.: Biogeohydrodynamic in the forested humid tropical environment: the case study of the Nsimi small experimental watershed (south Cameroon), Bull. la Société géologique Fr., 173(4), 347–357, 2002.

Braun, J.-J., Ngoupayou, J. R. N., Viers, J., Dupre, B., Bedimo, J.-P. B., Boeglin, J.-L., Robain, H., Nyeck, B., Freydier, R. and Nkamdjou, L. S.: Present weathering rates in a humid tropical watershed: Nsimi, South Cameroon, Geochim. Cosmochim.
530 Acta, 69(2), 357–387, 2005.

Braun, J.-J., Marechal, J.-C., Riotte, J., Boeglin, J.-L., Bedimo, J.-P. B., Ngoupayou, J. R. N., Nyeck, B., Robain, H., Sekhar, M. and Audry, S.: Elemental weathering fluxes and saprolite production rate in a Central African lateritic terrain (Nsimi, South Cameroon), Geochim. Cosmochim. Acta, 99, 243–270, 2012.

Brunet, F., Dubois, K., Veizer, J., Ndondo, G. R. N., Ngoupayou, J. R. N., Boeglin, J. L. and Probst, J. L.: Terrestrial and
535 fluvial carbon fluxes in a tropical watershed: Nyong basin, Cameroon, Chem. Geol., 265(3), 563–572, doi:https://doi.org/10.1016/j.chemgeo.2009.05.020, 2009.

Cardoso, S. J., Enrich-Prast, A., Pace, M. L. and Roland, F.: Do models of organic carbon mineralization extrapolate to warmer tropical sediments?, Limnol. Oceanogr., 59(1), 48–54, 2014.

Cole, J. J., Prairie, Y. T., Caraco, N. F., Mcdowell, W. H., Tranvik, L. J., Striegl, R. G., Duarte, C. M., Kortelainen, P.,
540 Downing, J. A., Middelburg, J. J. and Melack, J.: Plumbing the Global Carbon Cycle : Integrating Inland Waters into the Terrestrial Carbon Budget, Ecosystems, 10(1), 172–185, doi:10.1007/s10021-006-9013-8, 2007.

Deirmendjian, L. and Abril, G.: Carbon dioxide degassing at the groundwater-stream-atmosphere interface : isotopic equilibration and hydrological mass balance in a sandy watershed, J. Hydrol., 558, 129–143,

doi:10.1016/j.jhydrol.2018.01.003, 2018.

Deirmendjian, L., Loustau, D., Augusto, L., Lafont, S., Chipeaux, C., Poirier, D. and Abril, G.: Hydro-ecological controls on dissolved carbon dynamics in groundwater and export to streams in a temperate pine forest, Biogeosciences, 15(2), 669–691, doi:10.5194/bg-15-669-2018, 2018.

Deirmendjian, L., Anschutz, P., Morel, C., Mollier, A., Augusto, L., Loustau, D., Cotovicz, L. C., Buquet, D., Lajaunie, K., Chaillou, G., Voltz, B., Charbonnier, C., Poirier, D. and Abril, G.: Importance of the vegetation-groundwater-stream continuum to understand transformation of biogenic carbon in aquatic systems – A case study based on a pine-maize comparison in a lowland sandy watershed (Landes de Gascogne, SW France), Sci. Total Environ., doi:10.1016/j.scitotenv.2019.01.152, 2019.

DelSontro, T., Beaulieu, J. J. and Downing, J. A.: Greenhouse gas emissions from lakes and impoundments: Upscaling in the face of global change, Limnol. Oceanogr. Lett., 3(3), 64–75, doi:10.1002/lol2.10073, 2018.

Drake, T. W., Raymond, P. A. and Spencer, R. G. M.: Terrestrial carbon inputs to inland waters: A current synthesis of estimates and uncertainty, Limnol. Oceanogr. Lett., 3(3), 132–142, doi:10.1002/lol2.10055, 2018.

Gran, G.: Determination of the equivalence point in potentiometric titrations. Part II, Analyst, 77(920), 661–671, 1952.

Gumbricht, T., Román-Cuesta, R. M., Verchot, L. V, Herold, M., Wittmann, F., Householder, E., Herold, N. and Murdiyarso, D. A.-U. S. A. for I. D. (USAID): Tropical and Subtropical Wetlands Distribution version 2, , doi:doi:10.17528/CIFOR/DATA.00058, 2017.

Haase, K. and Rätsch, G.: The morphology and anatomy of tree roots and their aeration strategies, in Amazonian Floodplain Forests, pp. 141–161, Springer., 2010.

Hashimoto, S., Tanaka, N., Suzuki, M., Inoue, A., Takizawa, H., Kosaka, I., Tanaka, K., Tantasirin, C. and Tangtham, N.: Soil respiration and soil CO 2 concentration in a tropical forest, Thailand, J. For. Res., 9(1), 75–79, 2004.

Hotchkiss, E. R., Jr, R. O. H., Sponseller, R. A., Butman, D., Klaminder, J., Laudon, H. and Rosvall, M.: Sources of and processes controlling CO 2 emissions change with the size of streams and rivers, Nat. Geosci., 8(9), 696–699, doi:10.1038/NGEO2507, 2015.

Lafargue, E., Marquis, F. and Pillot, D.: Rock-Eval 6 applications in hydrocarbon exploration, production, and soil contamination studies, Rev. l'institut français du pétrole, 53(4), 421–437, 1998.

Lauerwald, R., Laruelle, G. G., Hartmann, J., Ciais, P. and Regnier, P. A. G.: Spatial patterns in CO2 evasion from the global river network, Global Biogeochem. Cycles, 29(5), 534–554, doi:10.1002/2014GB004941.Received, 2015.

Lehner, B., Verdin, K. and Jarvis, A.: New global hydrography derived from spaceborne elevation data, Eos, Trans. Am. Geophys. Union, 89(10), 93–94, 2008.

Lewis, E., Wallace Upton, NY (United States). Dept. of Applied Science], D. [Brookhaven N. L. and Allison TN (United States). Carbon Dioxide Information Analysis Center], L. J. [Oak R. N. L.: Program developed for CO{sub 2} system calculations, United States., 1998.

Liesack, W., Schnell, S. and Revsbech, N. P.: Microbiology of flooded rice paddies, FEMS Microbiol. Rev., 24(5), 625–645,

https://doi.org/10.5194/bg-2021-69
Preprint. Discussion started: 7 April 2021

2000.

Ludwig, W., Probst, J. and Kempe, S.: Predicting the oceanic input of organic carbon by continental erosion, Global Biogeochem. Cycles, 10(1), 23–41, 1996.

Maréchal, J., Braun, J., Riotte, J., Bedimo, J. B. and Boeglin, J.: Hydrological processes of a rainforest headwater swamp from natural chemical tracing in Nsimi watershed, Cameroon, Hydrol. Process., 25(14), 2246–2260, 2011.

Maurizot, P., Abessolo, A., Feybesse, J. L., Johan, V. and Lecomte, P.: Etude et prospection minière du Sud-Ouest Cameroun. Synthèse des travaux de 1978 à 1985, Rapp. BRGM 85 C., 66, 274p, 1986.

Meybeck, M.: Carbon, nitrogen, and phosphorus transport by world rivers, Am. J. Sci, 282(4), 401–450, 1982.

Meybeck, M.: Global chemical weathering of surficial rocks estimated from river dissolved loads, Am. J. Sci., 287(5), 401–428, doi:10.2475/ajs.287.5.401, 1987.

Millero, F. J.: The thermodynamics of the carbonate system in seawater, Geochem. Cosmochem. Ac., 43, 1651–1661, 1979.

Ndam Ngoupayou, J. R.: Bilans hydrogeochimiques sous foret tropicale humide en afrique: du bassin experimental de nesmi-zoetele aux reseaux hydrographiques du nyong et de la sanaga au sud-cameroun, Paris 6., 1997.

Nkoue-ndondo, G.-R.: Le cycle du carbone en domaine tropical humide: exemple du bassin versant forestier du Nyong au sud Cameroun, Université de Toulouse, Université Toulouse III-Paul Sabatier., 2008.

Nkoue-ndondo, G.-R., Probst, J.-L., Ndjama, J., Ngoupayou, J. R. N., Boeglin, J.-L., Takem, G. E., Brunet, F., Mortatti, J., Gauthier-Lafaye, F. and Braun, J.-J.: Stable Carbon Isotopes δ 13 C as a Proxy for Characterizing Carbon Sources and Processes in a Small Tropical Headwater Catchment: Nsimi, Cameroon, Aquat. Geochemistry, 1–30, 2020.

Nyeck, B., Bilong, P., Monkam, A. and Belinga, S. M. E.: Mise au point d'un modèle de cartographie et de classification des sols en zone forestières intertropicale au Cameroun. Cas du plateau forestier humide de Zoétélé, Géocam2, Press Uni. Yaoundé, 171–180, 1999.

Piedade, M. T. F., Ferreira, C. S., de Oliveira Wittmann, A., Buckeridge, M. and Parolin, P.: Biochemistry of Amazonian floodplain trees, in Amazonian floodplain forests, pp. 127–139, Springer., 2010.

Raich, J. W. and Schlesinger, W. H.: The global carbon dioxide flux in soil respiration and its relationship to vegetation and climate, Tellus B, 44(2), 81–99, 1992.

Raymond, P. A., Zappa, C. J., Butman, D., Bott, T. L., Potter, J., Mulholland, P., Laursen, A. E., Mcdowell, W. H. and Newbold, D.: Scaling the gas transfer velocity and hydraulic geometry in streams and small rivers, , 2, 41–53, doi:10.1215/21573689-1597669, 2012.

Raymond, P. A., Hartmann, J., Lauerwald, R., Sobek, S., McDonald, C., Hoover, M., Butman, D., Striegl, R., Mayorga, E., Humborg, C., Kortelainen, P., Dürr, H., Meybeck, M., Ciais, P. and Guth, P.: Global carbon dioxide emissions from inland waters, Nature, 503(7476), 355–359, doi:10.1038/nature12760, 2013.

Roden, E. E. and Wetzel, R. G.: Kinetics of microbial Fe (III) oxide reduction in freshwater wetland sediments, Limnol. Oceanogr., 47(1), 198–211, 2002.

Sanders, I. A., Cotton, J., Hildrew, A. G. and Trimmer, M.: Emission of Methane from Chalk Streams Has Potential

https://doi.org/10.5194/bg-2021-69
Preprint. Discussion started: 7 April 2021

Implications for Agricultural Practices, Freshw. Biol., 52(6), 1176–1186, doi:10.1111/j.1365-2427.2007.01745.x, 2007.

Sauer, D., Sommer, M., Jahn, R., Sauer, D., Sponagel, H., Sommer, M., Giani, L., Jahn, R. and Stahr, K.: Podzol : Soil of the Year 2007 . A review on its genesis , occurrence , and functions A review on its genesis , occurrence , and functions, J. Plant Nutr. Soil Sci., 170(5), 581–597, doi:10.1002/jpln.200700135, 2007.

Sharp, J. H.: The dissolved organic carbon controversy: an update, Oceanography, 6(2), 45–50, 1993.

Stanley, E. H., Casson, N. J., Christel, S. T., Crawford, J. T., Loken, L. C. and Oliver, S. K.: The ecology of methane in streams and rivers: Patterns, controls, and global significance, Ecol. Monogr., 86(2), 146–171, doi:10.1890/15-1027, 2016.

Strahler, A. N.: Mtm Quantitative Analysis of Watershed Geomorphology, Trans. Am. Geophys. Union, 38(6), 913–920, 1957.

Suchel, J.-B.: Les climats du Cameroun, Université de Bordeux III, France., 1987.

Toteu, S. F., Van Schmus, W. R., Penaye, J. and Michard, A.: New U–Pb and Sm–Nd data from north-central Cameroon and its bearing on the pre-Pan African history of central Africa, Precambrian Res., 108(1–2), 45–73, 2001.

Weiss, R. F.: Carbon dioxide in water and seawater: the solubility of a non-ideal gas, Mar. Chem., doi:10.1016/0304-4203(74)90015-2, 1974.

White, A. F. and Blum, A. E.: Effects of climate on chemical_ weathering in watersheds, Geochim. Cosmochim. Acta, 59(9), 1729–1747, 1995.

https://doi.org/10.5194/bg-2021-69
Preprint. Discussion started: 7 April 2021

Biogeosciences Discussions Open Access EGU

Rivers	Mengong	Mengong	Awout	So'o	Nyong	Nyong
Stations	Source	Outlet	Messam	Pont So'o	Mbalmayo	Olama
Latitude	3.17° N	3.17° N	3.28° N	3.32° N	3.52° N	3.43° N
Longitude	11.83° E	11.83° E	11.78°E	11.48° E	11.5 °E	11.28°E
Gauging station	No	Yes	Yes	Yes	Yes	Yes
Altitude (m)	680	669	647	634	634	628
Catchment area (km²)	0.48	0.6	206	3070	13,555	18,510
Wetlands (%)	NA	20	4.09	5.20	5.03	5.05
Catchment slope (‰)	1.3	1.3	1.2	1.1	0.16	0.15
Stream order	Groundwater	1	3	4	5	6
Averaged-annual river flow[a] ($m^3 s^{-1}$)	0.005[c]	0.009	4	36	145	195
Averaged-annual rainfall[b] (mm an^{-1})	1779	1779	1779	1749	1759	1631

Table 1: geographical and hydrological catchments characteristics. [a]During the year 2016. [b] From Brunet et al. (2009). [c]From Maréchal et al. (2011).

30

https://doi.org/10.5194/bg-2021-69
Preprint. Discussion started: 7 April 2021

Parameters	T	pH	Conductivity	O_2	TSM
Units	°C	unitless	µS cm^{-1}	%	mg L^{-1}
Mengong source	23.2±0.1	5.0±0.1	15.1±0.8	50±8	NA
	[23~23.6]	[4.6~5.3]	[14.1~17.4]	[38~68]	NA
Mengong outlet	22.9±0.7	5.6±0.2	16.7±4.5	50±9	5.3±2.1
	[21.9~24.4]	[5.3~6.0]	[5.2~24.7]	[23~62]	[1.8~11.1]
Awout	22.5±0.5	5.6±0.2	21.6±5.5	47±9	10.4±6.1
	[22~23.5]	[5.04~6.1]	[16.5~40.3]	[37~67]	[4.9~27.5]
So'o	23.9±1.3	6.1±0.2	23.4±5.0	57±6	14.4±3.8
	[22.4~27.6]	[5.7~6.6]	[18.3~35]	[46~69]	[8.2~22.9]
Nyong (Mbalamayo)	26.1±1.3	6.2±0.3	36.6±19	40±20	8.9±2.0
	[24.3~29.0]	[5.5~6.9]	[19.6~86.3]	[13~81]	[4.3~12.0]
Nyong (Olama)	25.7±1.4	6.2±0.3	31.4±12.8	43±12	9.7±3.2
	[24.1~28.8]	[5.5~6.6]	[20.1~69.3]	[24~67]	[3.7~14.8]

Table 2: Spatial distribution of physicochemical parameters (mean ± standard deviation) in rivers of the Nyong basin during the sampling period. The range is shown in square brackets.

https://doi.org/10.5194/bg-2021-69
Preprint. Discussion started: 7 April 2021

Biogeosciences Discussions Open Access EGU

Parameters	pCO_2	TA	DIC	DOC	POC	POC
Units	ppmv	µmol L^{-1}	µmol L^{-1}	µmol L^{-1}	%	µmol L^{-1}
Mengong source	78800±40110	53±26	2940±1485	108±10[a]	NA	NA
	[12700~209000]	[15~138]	[500~7560]	NA	NA	NA
Mengong outlet	15600±8900	90± 36	670±360	1925±970	23±5	101±44
	[3980~41000]	[20~156]	[170~1710]	[1090~4150]	[14~26]	[14~213]
Awout	15400±7300	67±39	670±315	3200±1840	16±3	130±50
	[5760~26710]	[11~166]	[260~1170]	[2000~7550]	[11~21]	[72~243]
So'o	12700±5100	74±34	670±260	2170±980	18±4	210±60
	[4900~23200]	[10~145]	[300~1320]	[1100~5320]	[12~29]	[125~360]
Nyong (Mbalamayo)	11800±5100	123±63	720±270	2000±860	20±3	150±40
	[3620~22460]	[20~230]	[220~1200]	[1020~5300]	[16~26]	[62~220]
Nyong (Olama)	11000±5550	134±70	640±330	1860±440	18±2	150±50
	[3000~21700]	[10~265]	[170~1240]	[1100~2880]	[15~23]	[55~235]

Table 3: Spatial distribution of dissolved and particulate C concentrations (mean ± standard deviation) in rivers of the Nyong basin during the sampling period. The range is shown in square brackets.. [a]From Brunet et al. (2009).

https://doi.org/10.5194/bg-2021-69
Preprint. Discussion started: 7 April 2021

Biogeosciences Discussions Open Access EGU

.

	F_{respi}	k_{600}	CO_2^*	F_{degas}	Water surface area	F_{degass_CO2}
	mmol m^{-2} d^{-1}	m d^{-1}	µmol L^{-1}	mmol m^{-2} d^{-1}	km²	Gg C yr^{-1}
1	15±11 (36[a])	2.2	564	1235	7.7	42
2		2.7	564	1469	19.3	126
3		3.1	563	1694	20.1	149
4		3.1	433	1311	23.2	133
5	120±120 (141[a])	2.4	395	913	26.0	104
6		2.5	384	934	40.3	165
Total						718[b] (*25.8*[c])

Table 4: C degassing at the water-air interface and pelagic respiration. Fluxes in mmol m^{-2} d^{-1} are related to the water surface area. [a] taking into account an additional benthic respiration of 21 mmol m^{-2} d^{-1}. [b] calculated from the sum of C degassing (Gg C yr^{-1}) in each stream order. [c] in t C km^{-2} yr^{-1}, which fluxes are weighed by the surface area of the entire Nyong basin.

50

https://doi.org/10.5194/bg-2021-69
Preprint. Discussion started: 7 April 2021

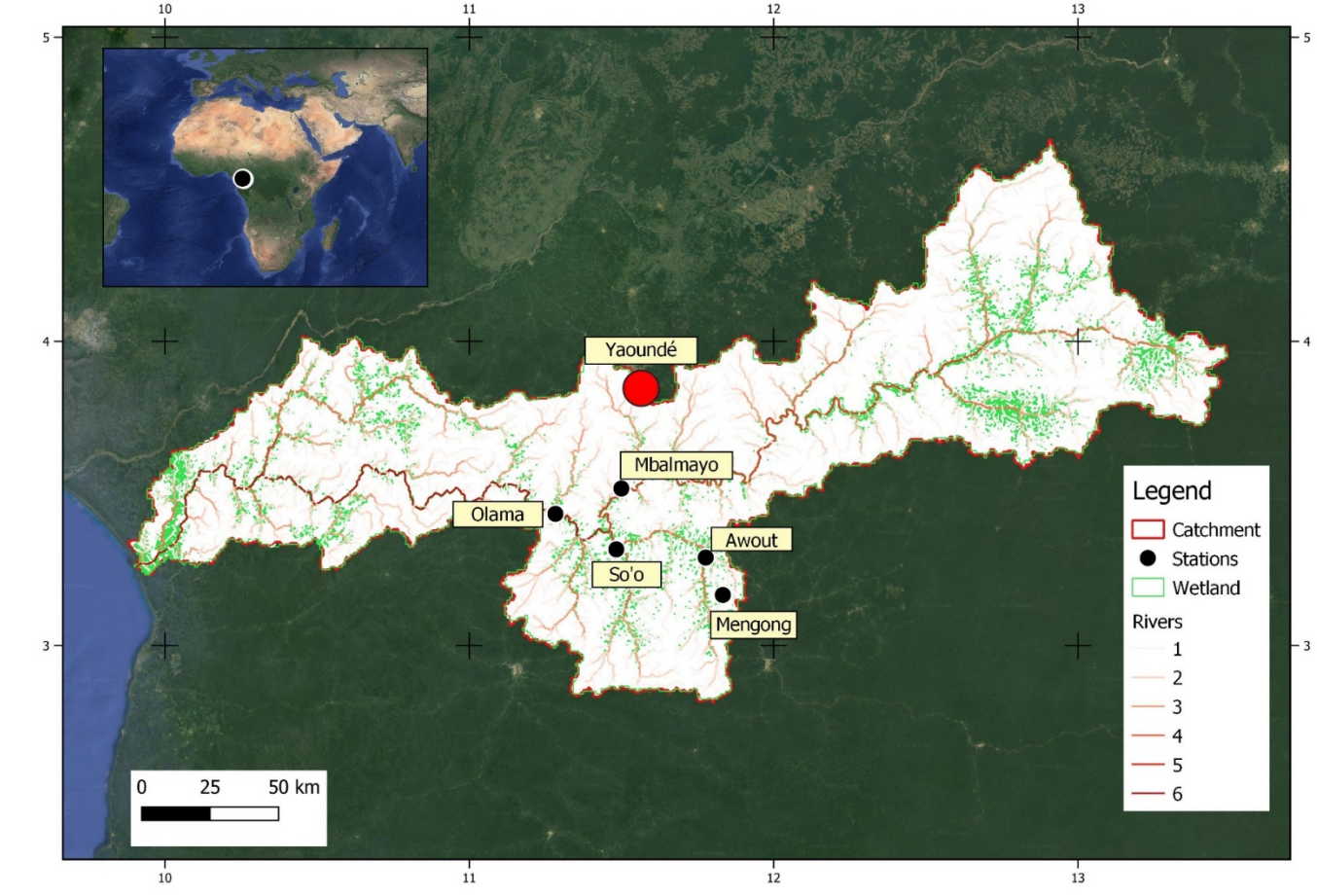

Figure 1: Figure 1: Map of the Nyong catchment showing location of the sampling sites, the different sub-catchments and the river network. The map was done with QGis Software.

https://doi.org/10.5194/bg-2021-69
Preprint. Discussion started: 7 April 2021

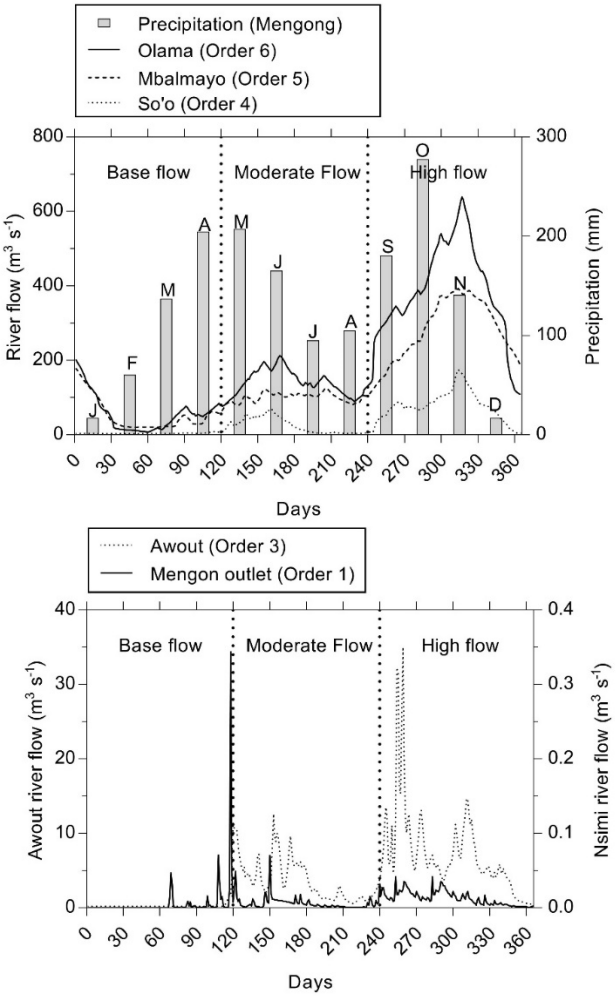

Figure 2: River flows of the different gauging stations during the year 2016, associated with precipitation measured at the Mengong catchment.

https://doi.org/10.5194/bg-2021-69
Preprint. Discussion started: 7 April 2021

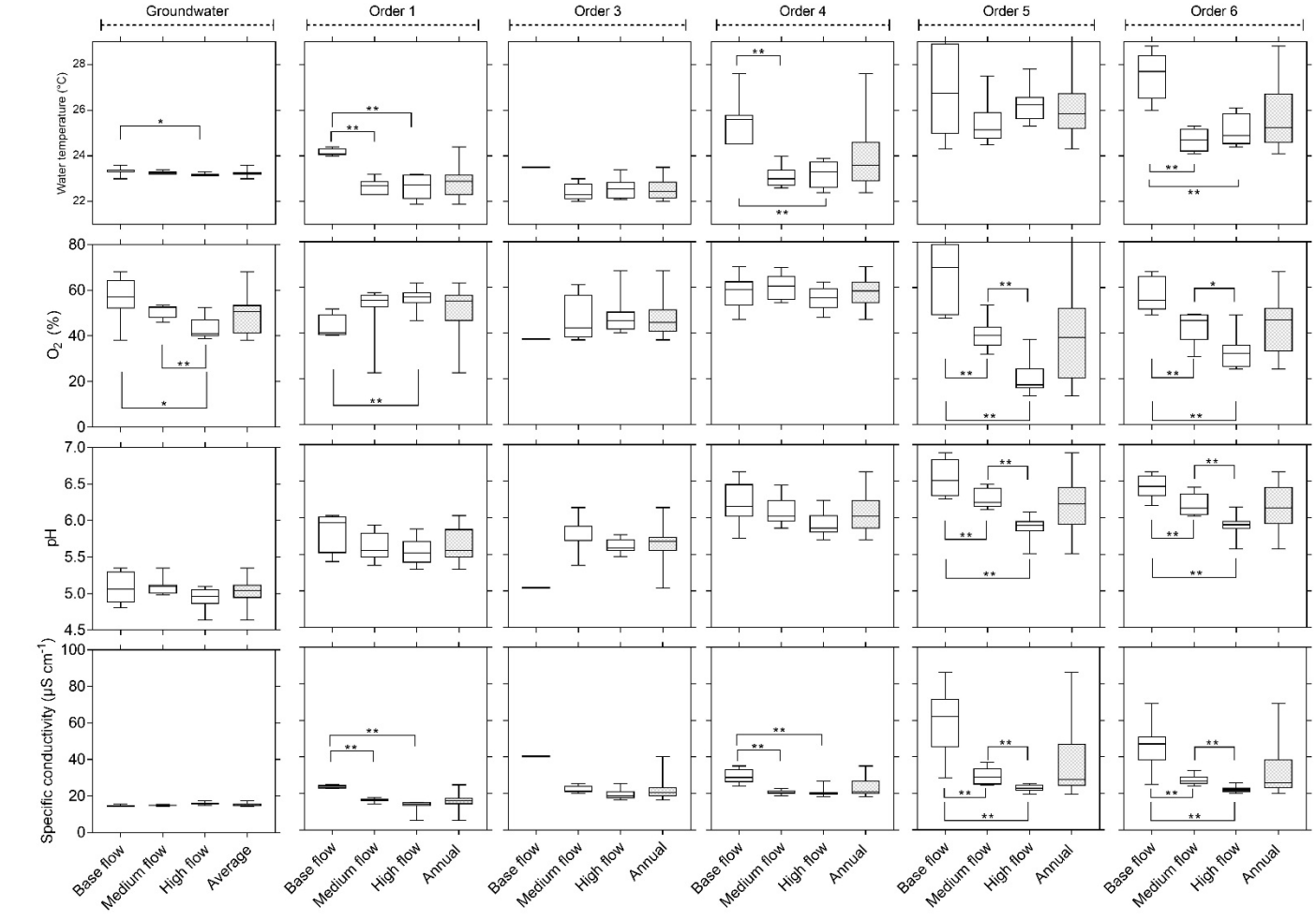

Figure 3: Box plots showing the seasonal (related to the river flow) and the spatial (related to stream order) variations of water temperature (°C), O_2 (%), pH and specific conductivity (µS cm^{-1}). One star (*) and two stars (**) indicate a p value <0.05 and <0.001, respectively.

https://doi.org/10.5194/bg-2021-69
Preprint. Discussion started: 7 April 2021

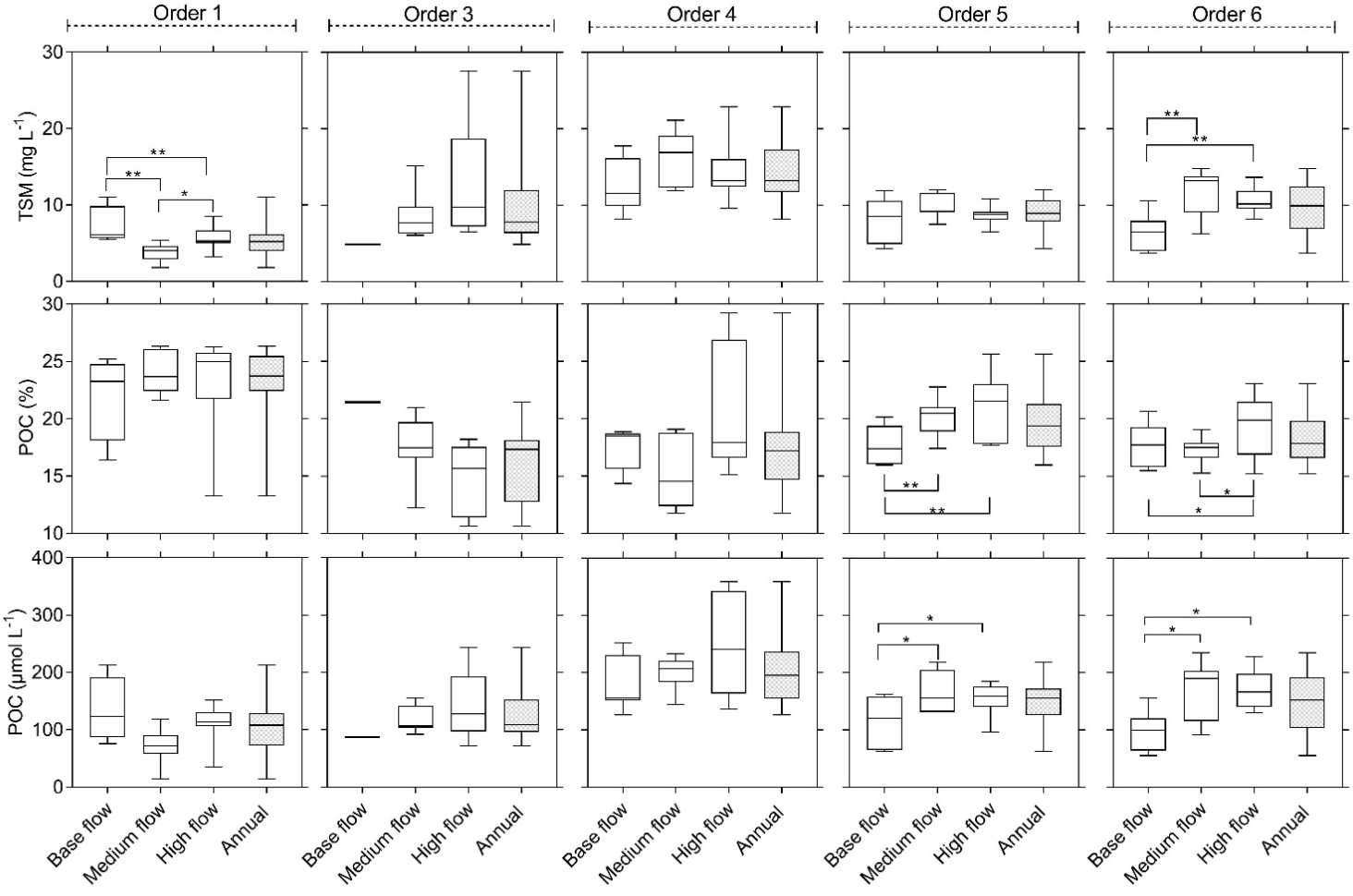

Figure 4: Box plots showing the seasonal (related to the river flow) and the spatial (related to stream order) variations of TSM (mg L^{-1}), the POC content of the TSM (POC%, %) and POC (µmol L^{-1}). One star (*) and two stars (**) indicate a p value <0.05 and <0.001, respectively.

https://doi.org/10.5194/bg-2021-69
Preprint. Discussion started: 7 April 2021

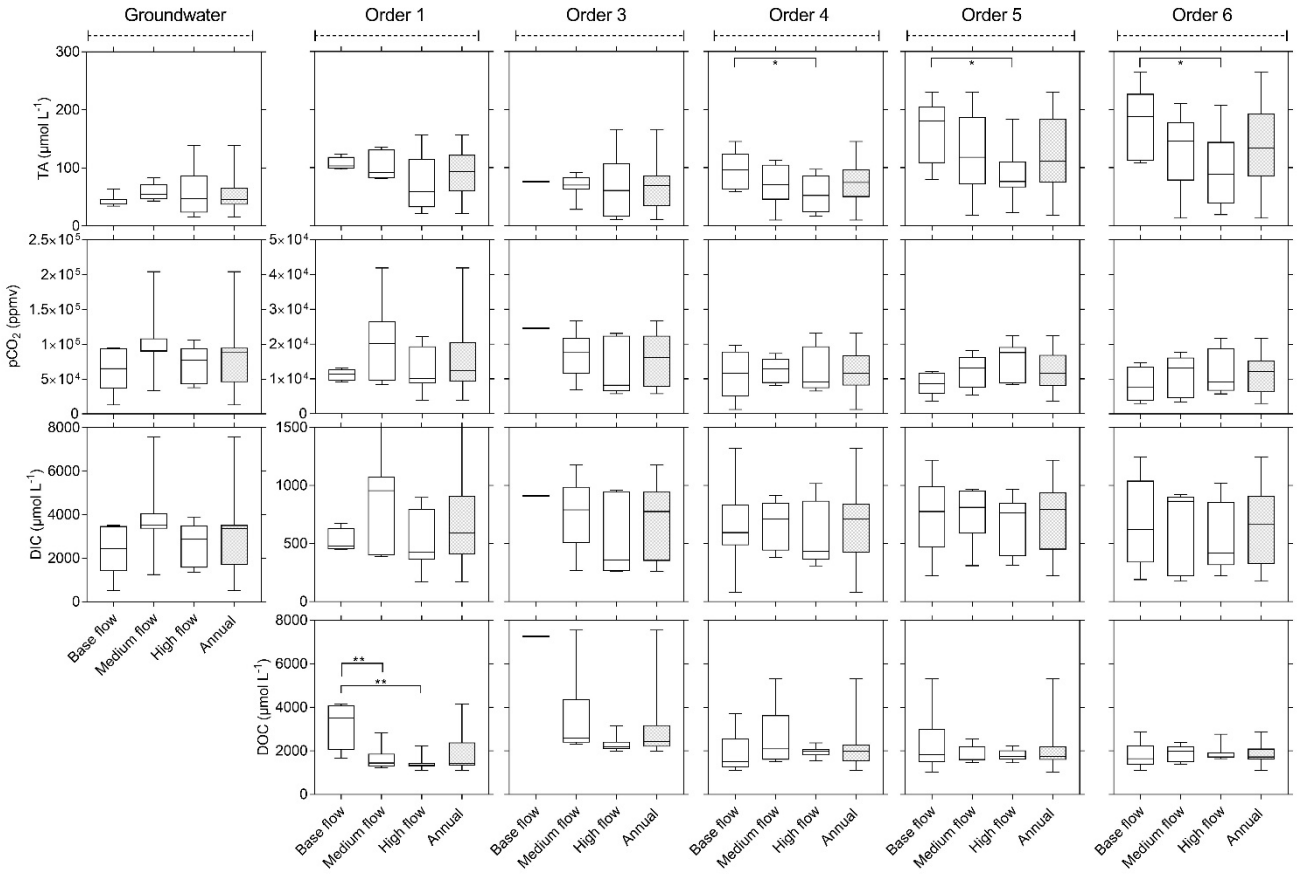

Figure 5: Box plots showing the seasonal (related to the river flow) and the spatial (related to stream order) variations TA (µmol L^{-1}), pCO_2 (ppmv), DIC (µmol L^{-1}) and DOC (µmol L^{-1}). One star (*) and two stars (**) indicate a p value <0.05 and <0.001, respectively.

https://doi.org/10.5194/bg-2021-69
Preprint. Discussion started: 7 April 2021

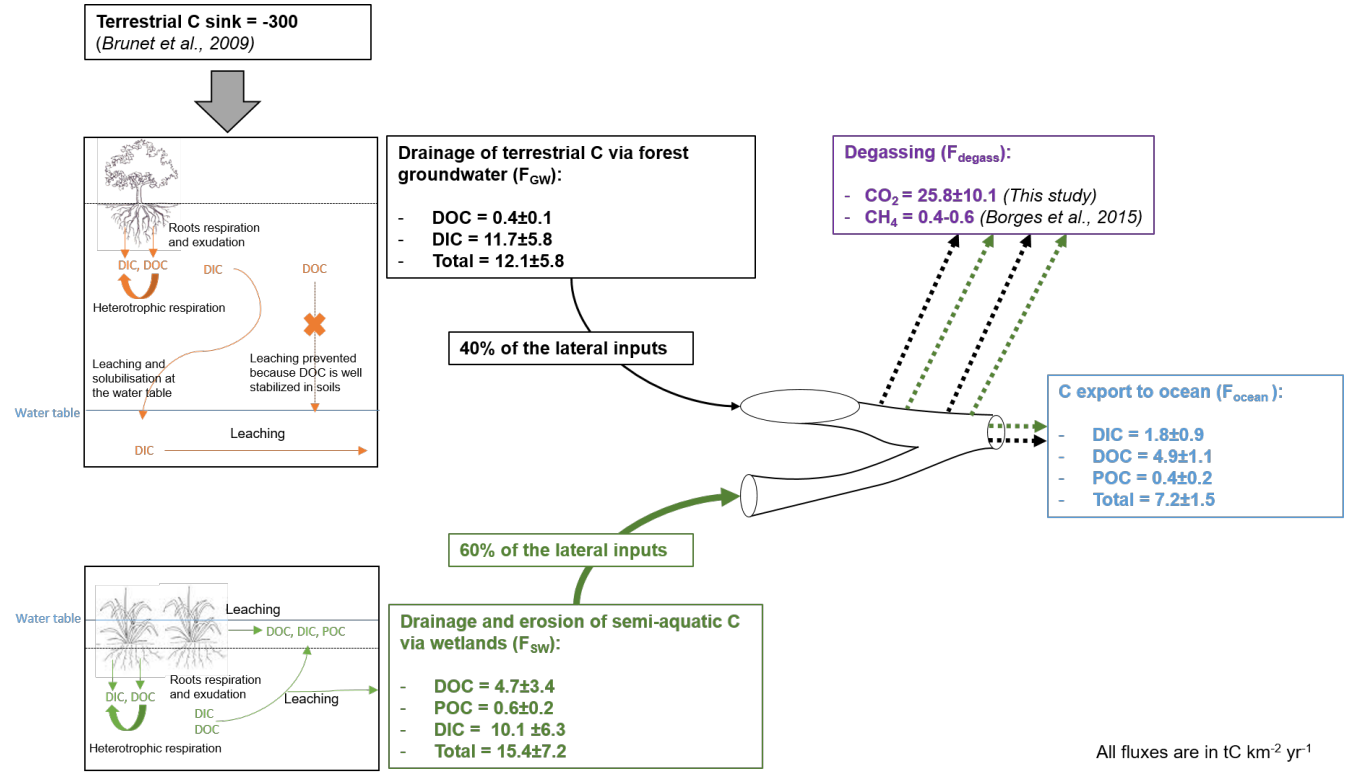

Figure 6: Eco-hydrological processes occurring in wetlands and forest groundwater associated with the riverine carbon budget at the catchment scale.

690